Magnon Pairs and Spin-Nematic Correlation in the Spin Seebeck Effect

Daichi Hirobe,[1,*] Masahiro Sato,[2,3,†] Masato Hagihala,[4,5] Yuki Shiomi,[6] Takatsugu Masuda,[4] and Eiji Saitoh[1,2,7,8]
[1]*Institute for Materials Research, Tohoku University, Sendai 980-8577, Japan*
[2]*Spin Quantum Rectification Project, ERATO, Japan Science and Technology Agency, Sendai 980-8577, Japan*
[3]*Department of Physics, Ibaraki University, Mito, Ibaraki 310-8512, Japan*
[4]*Institute of Solid State Physics, The University of Tokyo, Kashiwa, Chiba 277-8581 Japan*
[5]*Institute of Materials Structure Science, High Energy Accelerator Research Organization (KEK), Tokai, Ibaraki 319-1106, Japan*
[6]*Department of Basic Science, University of Tokyo, Meguro, Tokyo 153-8902, Japan*
[7]*The Advanced Science Research Center, Japan Atomic Energy Agency, Tokai 319-1195, Japan*
[8]*WPI Advanced Institute for Materials Research, Tohoku University, Sendai 980-8577, Japan*

(Received 11 April 2019; published 12 September 2019)

Investigating exotic magnetic materials with spintronic techniques is effective at advancing magnetism as well as spintronics. In this work, we report unusual field-induced suppression of the spin Seebeck effect (SSE) in a quasi-one-dimensional frustrated spin-$\frac{1}{2}$ magnet $LiCuVO_4$, known to exhibit spin-nematic correlation in a wide range of external magnetic field B. The suppression takes place above $|B| \gtrsim 2$ T in spite of the B-linear isothermal magnetization curves in the same B range. The result can be attributed to the growth of the spin-nematic correlation while increasing B. The correlation stabilizes magnon pairs carrying spin 2, thereby suppressing the interfacial spin injection of SSE by preventing the spin-1 exchange between single magnons and conduction electrons at the interface. This interpretation is supported by integrating thermodynamic measurements and theoretical analysis on the SSE.

DOI: 10.1103/PhysRevLett.123.117202

Introduction.—Spin Seebeck effects (SSE) [1–19] refer to the generation of a spin current owing to a temperature gradient in a magnetic material. It takes place in a magnetic insulator with a metallic contact. When nonequilibrium magnons are accumulated at the interface due to a temperature gradient, the annihilation of such a single magnon is followed by the flip of a conduction-electron spin via the interfacial exchange interaction. As a result, the exchange of spin 1 takes place dominantly, enabling conversion from a magnon spin current into a conduction-electron one [3]. The latter spin current can be detected as a transverse electric field via the inverse spin-Hall effect [20–23] in the metallic contact. SSEs have been found to take place even in paramagnetlike insulators with spin correlations [16–18]. These findings point to the use of SSE as a probe for spin correlations without the magnetic orders, for example, in quantum spin systems [24–27].

The magnetic quadpolar correlation, also known as the spin-nematic correlation [28–30], is the simplest example of magnetic multipolar correlations. It represents the correlation between magnon pairs, rather than single magnons. To stress this point, the spin-nematic correlation will be called the magnon-pair correlation hereafter. A typical magnon-pair correlation appears in a one-dimensional (1D) frustrated spin-$\frac{1}{2}$ chain with the ferromagnetic nearest neighboring exchange interaction $J_1 < 0$ and the antiferromagnetic next nearest neighboring one $J_2 > 0$. The Hamiltonian of this 1D J_1-J_2 model reads

$$\mathcal{H} = \sum_j (J_1 \boldsymbol{S}_j \cdot \boldsymbol{S}_{j+1} + J_2 \boldsymbol{S}_j \cdot \boldsymbol{S}_{j+2} - g\mu_B B S_j^z). \quad (1)$$

Here, $\boldsymbol{S}_j$ is the spin-$\frac{1}{2}$ operator on the jth site, and the site number j increases along the spin-chain direction. The last term represents the Zeeman interaction with the external magnetic field B along the z axis with g and μ_B being, respectively, the g factor and the Bohr magneton. The low-energy physical properties of Eq. (1) and its variants have been elucidated [31–36] using powerful theoretical techniques in the last decade. The ground-state diagram with $|J_1/J_2| = \mathcal{O}(1)$ [32,33] is schematically shown in Fig. 1(a) as a function of B. In the lower B range, a Tomonaga-Luttinger liquid (TLL) [27] with a vector spin chirality [37–41] appears. As B is increased, the magnon-pair correlation grows to give rise to a spin-nematic TLL [31–36] in a wide B range. In this state, single magnons acquire an energy gap equivalent to the binding energy of magnon pairs while magnon pairs are gapless. Accordingly, a change in spin angular momentum is quantized in units of $2\hbar$, not $\hbar$, in low energy.

In this study, we have investigated the SSE in an insulating quantum magnet $LiCuVO_4$ [42–45]. $LiCuVO_4$ is an established model material for a strong magnon-pair correlation, representing a family of quasi-1D $J_1 - J_2$ magnets [46–54]. Since the spin quantum number carried by quasiparticles is increased effectively by magnon-pair formation, the SSE seems to be enhanced while increasing B. Contrary to this naïve expectation, the SSE in $LiCuVO_4$

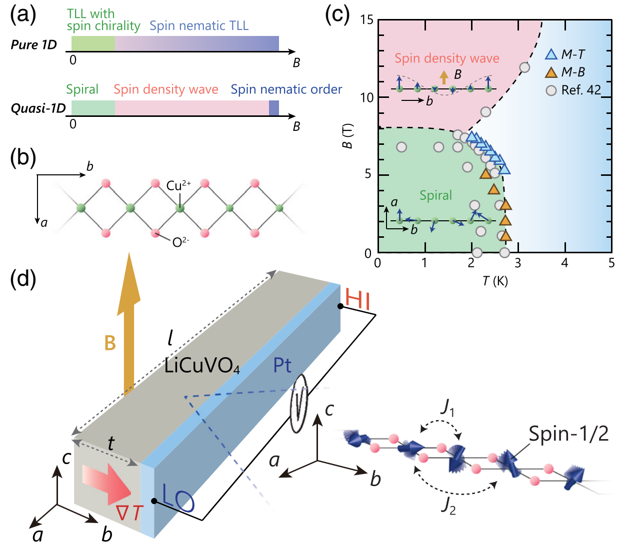

FIG. 1. (a) Theoretical ground-state phase diagrams of a purely 1D frustrated J_1-J_2 spin-$\frac{1}{2}$ chain [32,33] (top) and a quasi-1D one with an interchain exchange interaction [36] (bottom). B denotes external magnetic field. (b) Spin chain in $LiCuVO_4$ composed of Cu^{2+} and O^{2-} ions. (c) Magnetic field (B)—temperature (T) phase diagram of $LiCuVO_4$, obtained while applying B in the c axis. Triangular data points were taken in this study: the sky-blue ones from the T dependence of the magnetization M, the orange ones from the B dependence of M. The circular data points were adapted from Ref. [42]. (d) Experimental setup for detecting the spin-Seebeck effect in a $LiCuVO_4$/Pt system. J_1 and J_2, respectively, denote the nearest and next-nearest-neighboring exchange interactions in the spin chain of $LiCuVO_4$; ∇T a temperature gradient along the spin chain; t and l, respectively, the thickness and the length of the $LiCuVO_4$.

has been observed to exhibit a strong B-induced suppression alongside the B-linear magnetization curves above the magnetic ordering temperatures. Such a B response of the SSE is different from those of magnetically ordered states [1,12–14] and a 1D quantum spin liquid [16]. We interpret the result as the evidence for B-induced crossover from the single-magnon correlation to the magnon-pair one, and its resulting prevention of the interfacial exchange of spin 1 in the SSE. Observing the magnon-pair correlation is generally difficult. Our study shows that SSE serves as a powerful probe for dynamical and transport natures of such spin-nematic states in quantum magnets.

Spin-nematic nature of $LiCuVO_4$.—$LiCuVO_4$ is a typical Mott insulator for which experimental evidences for the magnon-pair correlation have been established. A spin chain embedded in $LiCuVO_4$ is shown in Fig. 1(b). Each Cu^{2+} ion carries spin-$\frac{1}{2}$ and they form a 1D chain along the b axis by sharing O^{2-} ions. If the weak interchain interaction J' is ignored, $LiCuVO_4$ can be well described by Eq. (1). The magnitudes of J_1 and J_2 were estimated experimentally, for example, from neutron scattering spectra [43,45,55,56]: $J_2 = 40$–70 K and $|J_1/J_2| = \mathcal{O}(1)$. Because of the weak J' in $LiCuVO_4$, magnetically ordered phases appear at low temperatures; however, each phase nicely reflects the phase diagram of the purely 1D model [see also Fig. 1(a)]. J' was estimated experimentally to be a few Kelvin [43,45], consistent with the magnetic ordering temperatures (T_c) of about 3 K [42–45]. In a low-B range below T_c, a spin spiral order appears [39,42,44], reflecting the TLL with a vector spin chirality [39–41]. As B is increased to about 7 T, a spin-density-wave (SDW) order appears as shown in Fig. 1(c), and it continues up to about 50 T ($\sim J_2$). Immediately below the saturation magnetization, a three-dimensional (3D) spin-nematic order may occur [36,57–59], whose possible existence attracts attention. Importantly, the magnon-pair (spin-nematic) correlation evidently persists above T_c, and exhibits a quasi long-range order over a wide B range together with the SDW correlation. In Refs. [34,35], a theoretical proposal was made for detecting signs of the spin-nematic TLL by nuclear magnetic resonance (NMR) and neutron scattering techniques, followed by experimental observations of those signs [60–63].

Experimental details.—Single crystals of $LiCuVO_4$ were grown by a traveling-solvent floating-zone method, which was exactly the same as reported by one of the present authors [62]. The grown single crystals were cut into cuboids that were typically 5 mm along the a axis and 1 mm along the b and c axes for SSE measurements. Temperature (T) and magnetic field (B) dependences of the magnetization were found to be consistent with a B–T phase diagram reported elsewhere [42], as shown in Fig. 1(c). The experimental details and the magnetic properties are described in the Supplemental Material [64].

We used a $LiCuVO_4$/Pt junction system as shown in Fig. 1(d) to investigate the SSE. A temperature gradient ∇T was applied along the spin chains with a heater. We created the temperature difference ΔT between the top of the Pt film and the rear of the $LiCuVO_4$. Au wires were attached to the ends of the Pt film to obtain the dc voltage V, for which we excluded a background voltage signal taken with the heater off. The magnetic field B was applied along the c axis, being perpendicular both to ∇T and the direction across the electrodes; thus, the c axis corresponds to the z axis in Eq. (1) while the a and b axes to the x and y axes, respectively. To quantitatively compare the voltage signals, we show the transverse thermopower $S = j_e/|\nabla T| \approx (V/\Delta T\rho)(t/l)$. Here j_e is the current density in the Pt film due to thermoelectric effects, ρ is the electrical resistivity of the Pt film, and t and l are, respectively, the thickness and the length of the $LiCuVO_4$. Additionally, we defined the average temperature T_{ave} as $T_{\mathrm{ave}} = (T_H + T_L)/2$ in which $T_H = T + \Delta T$ and $T_L = T$ are, respectively, the temperatures of the top of the Pt film and the rear of the $LiCuVO_4$. The experimental details of SSE measurements are described in Supplemental Material [64].

Experimental results for SSE.—In Figs. 2(a) and 2(b), we show the B dependence of the transverse thermopower S at

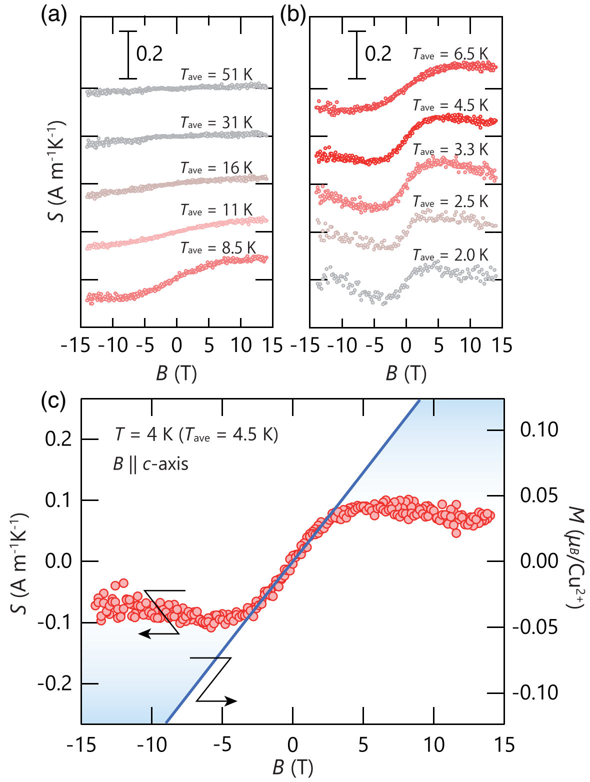

FIG. 2. (a),(b) B dependence of the transverse thermopower S at several T. (c) Comparison between B dependences of S and M at $T = 4$ K.

several $T_{\rm ave}$. A small S was detected at 51 K, and found to be B linear. This can be explained by the normal Nernst effect of Pt [7,16]. However, as $T_{\rm ave}$ is decreased down to 11 K, a clear signal appears. Its sign reverses when the magnetization is reversed, which is a typical feature of SSE. Interestingly, S starts deviating from a B-linear line, and decreases while increasing B. As shown in Fig. 2(b), the deviation enhances with a further decrease of $T_{\rm ave}$ down to 2 K, the lowest temperature in this study.

To look into this B dependence of S in more detail, we compare the B dependences of S and the magnetization M at $T = 4$ K in Fig. 2(c). Remarkably, in spite of the B-linear change in M, S gets suppressed strongly while increasing B, and even exhibits a negative slope at $|B| \gtrsim 5$ T. We stress that the suppression of S cannot be attributed to magnetic phase transitions since it takes place even above T_c [see also Fig. 1(c)]. Additionally, the Zeeman energy gap in spin excitations is unlikely to explain the B-induced suppression of S although seemingly similar results were reported for ferrimagnets and paramagnets [8,9,18]. Generally the Zeeman energy gap starts suppressing thermal magnetic excitations as the magnetization approaches saturation at low temperatures. Since M of $LiCuVO_4$ is B linear alongside $\sim 0.1\,\mu_B/Cu^{2+}$ even at $B = 9$ T, the smooth $M - B$ curve indicates the existence of a gapless magnetic excitation [78–80].

The unusual suppression of S invokes the magnon-pair correlation, which yields magnon pairs with a binding energy $E_{\rm bind}$. $E_{\rm bind}$ has been predicted to already exist near zero magnetic field [36]. Figure 3(a) shows the calculated B dependence of $E_{\rm bind}$ for a purely 1D case with $|J_1/J_2| = 1$ [36]. $E_{\rm bind}$ increases linearly with B alongside the B-linear magnetization when B is much lower than the saturation field [see also the inset to Fig. 3(a)]. Within this framework, the B-induced $E_{\rm bind}$ stabilizes magnon pairs while inhibiting thermal excitation of single magnons. Because spin injection of SSE at the interface stems mainly from the exchange of spin-1, spin-2 magnon pairs cannot contribute to such spin injection, thereby decreasing SSE signals. The ability to selectively probe spin-1 magnetic excitations should differentiate SSE measurements from thermal conductivity measurements. This is because the latter measurements simultaneously probe phonons as well as multiple magnetic excitations carrying spin 1 and spin 2 [64].

Comparison between experimental and theoretical results.—We theoretically calculate spin currents injected from a magnet ($LiCuVO_4$) to a metal (Pt) and compare them with S, because inverse spin-Hall voltages are proportional to injected spin currents. For simplicity, we assume that the spin dynamics of $LiCuVO_4$ is described by a spin-nematic TLL, ignoring the weak interchain interactions. We also make the conventional assumption that a weak exchange interaction $J_{\rm sd}$ exists at the interface between the magnet and the metal. The normalized spin current $\tilde{J}_s$ [3,16,81] is then given by (see Supplemental Material [64])

$$\tilde{J}_s = \frac{1}{T^2}\int d\omega \,{\rm Im}\chi^{-+}_{\rm mag}(\omega, T)\frac{\omega^2}{1+\tau_s^2\omega^2}\frac{1}{\sinh^2[\omega/(2T)]}, \quad (2)$$

up to the leading order of $J_{\rm sd}$. Here, ω is the angular frequency, T is the mean value of the two temperatures of the magnet and the metal, and τ_s is the spin relaxation time for the metal. The integral range is $(-\infty, \infty)$. $\chi^{-+}_{\rm mag}$ denotes the dynamical spin susceptibility of the magnet, and describes the dynamics of a single magnon (strictly speaking, a paramagnon in a spin-nematic TLL). In Eq. (2) the spin current is injected by single magnons which have an energy gap due to magnon-pair formation. We have ignored the magnon-pair-driven spin current considering its small magnitude [64]. Magnon-pair formation is considered via the resulting energy gap in $\chi^{-+}_{\rm mag}$ whose low-energy form at finite temperatures was determined within the framework of practical approximation.

In Fig. 3(b), we show the B dependences of calculated $\tilde{J}_s$ and measured S at $T = 4$ K normalized by their maximum values. We set $J_1/J_2 = -1$ and $J_2 = 50$ K in the calculation and normalized B by the saturation field B_s (see also the caption of Fig. 3). $\tilde{J}_s$ and S increase linearly with B near zero magnetic field. This can be attributed to the growth of the uniform ferromagnetic moment and the angular

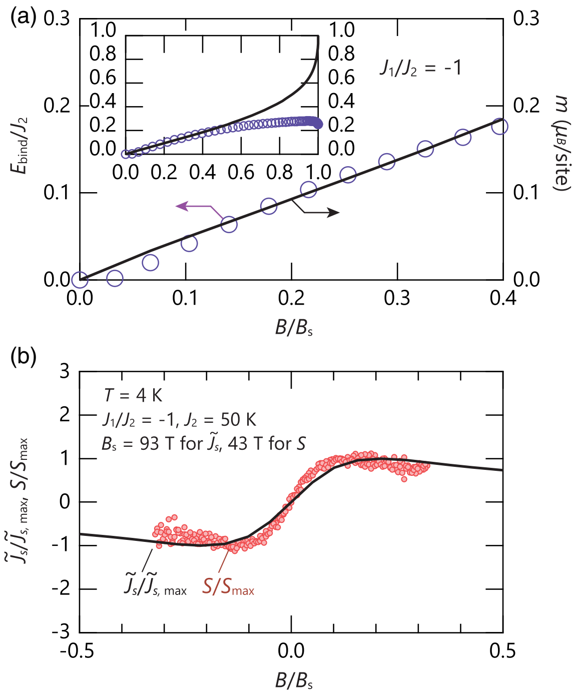

FIG. 3. (a) B dependences of the magnon-pair binding energy E_{bind} and the calculated magnetic moment per site $m = 2\langle S_j^z \rangle$ for a 1D frustrated spin chain with $J_1/J_2 = -1$ [see also Eq. (1)] [36]. The inset shows the B dependences up to $B/B_s = 1$ with B_s being the saturation field. (b) B dependence of the calculated spin current $\tilde{J}_s$ injected into a metal by single magnons which have an energy gap equal to the magnon-pair binding energy. The B dependence of S is also shown as data points for comparison. B is normalized by $B_s = 93$ T for $\tilde{J}_s$, calculated with $J_1/J_2 = -1$ and $J_2 = 50$ K while by $B_s \sim 43$ T for S [45,59]. $\tilde{J}_s$ and S are, respectively, normalized by their maximum values $\tilde{J}_{s,\max}$ and $S_{\max}$.

momentum along B per single magnon [82]. Most importantly, $\tilde{J}_s$ starts to be suppressed upon a further increase of B, and exhibits a broad peak structure around $|B| = 9$ T, capturing the marked feature of S observed experimentally. Since applying B of this magnitude yields $E_{\mathrm{bind}} \sim 3$ K [see also Fig. 3(a)], the B-induced suppression at $T = 4$ K can be ascribed to a decrease in thermally excited single magnons that is induced by magnon-pair formation. We stress that the theoretical B_s is varied easily by changing J_1 and J_2 [32] in the spin-nematic TLL state while the B linearity of E_{bind} is not [36]. Thus, the B dependence of $\tilde{J}_s$ little depends on change of B_s. This indicates that a difference between the theoretical $B_s = 93$ T and the experimental $B_s \sim 43$ T is not essential in reproducing the characteristic B dependence of S.

We note that for $LiCuVO_4$, the 3D spin spiral correlation likely coexists with the magnon-pair one above magnetic ordering temperatures ~3 K [see also Fig. 1(c)]. Since B is applied parallel to the spiral axis along the c axis, the low-B SSE is similar to antiferromagnetic SSEs in canted phases [12,13]. In these previous cases, spin Seebeck coefficients exhibit positive sign along with the same B dependences as those of M. These features are expected to be embedded in our low-B SSE results. Integrating such effects into the above calculation will yield a more quantitative result while the B-induced suppression of magnon-pair origin should carry over.

In Fig. 4, we compare the T_{ave} dependences of S for several B with our theoretical calculations, in which finite-temperature effects on the single-magnon dynamics are considered besides the magnon-pair binding energy. When B is below ~5 T, S only saturates toward low T_{ave} as seen in Fig. 4(a). However, when B is above ~5 T, a broad peak structure emerges, and its peak position gradually shifts from ~5 to ~8 K while increasing B to 14 T. These temperature dependences are also successfully captured by our calculation based on Eq. (2), as shown in Fig. 4(b). This shows that the broad peaks stem from the competition between a decrease in the single-magnon density due to the magnon-pair formation and an increase in the single-magnon lifetime at low temperatures. Additionally, the agreement between Figs. 4(a) and 4(b) indicates that the peak shift caused by increasing B could be attributed to an increase in the angular momentum along B per single magnon [82]: Such increased angular momentum enhances SSE at high temperature where the B-induced magnon-pair binding energy can be overcome by thermal fluctuation; otherwise, SSE is decreased more greatly toward low temperature via magnon-pair formation. This can be responsible for the peak shift observed in Fig. 4(a). Overall, the agreement between the experimental and theoretical results shows that the B and T dependences of S can be well explained by magnon-pair formation. We also note that our results point to exchange of spin 1 as the most relevant magnetic interaction at the interface in SSE.

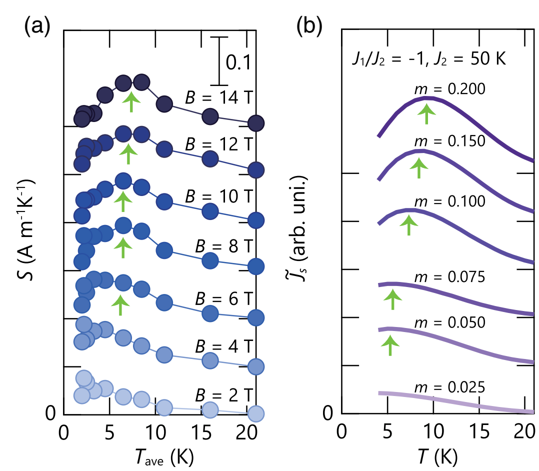

FIG. 4. (a) T_{ave} dependence of S at several B. Datasets are shifted by multiples of 0.1 A $\mathrm{m^{-1}\,K^{-1}}$. (b) T dependence of the calculated spin current $\tilde{J}_s$ that is injected into a metal by single magnons with an energy gap equal to the magnon-pair binding energy. $m = 2\langle S_j^z \rangle$ is the magnetic moment per site.

Summary.—We observed the magnetic-field-induced suppression of the SSE in a quasi-1D frustrated spin-chain system $LiCuVO_4$, an established model material for the spin-nematic correlation. A broad peak structure was also found to appear in the temperature dependence of the spin-Seebeck voltage, and to shift toward high temperatures while increasing magnetic field. These experimental results were well reproduced by a microscopic calculation of the interfacial spin current where the magnon-pair binding energy and its resulting energy gap of the single magnons are taken into consideration. Our result indicates that SSE is a powerful tool for detecting signatures of spin-nematic states and their transport properties.

We thank Toshiya Hikihara for fruitful discussion on the magnon-pair binding energy. We also thank Takashi Kikkawa for experimental assistance. This work is supported by JSPS (KAKENHI No. 17H04806, No. 18H04215, No. 18H04311, No. 18H05854, No. 19H02424, No. 19K22124, No. 19H05600, and No. 26247058 and the Core-to-Core program "International research center for new-concept spintronics devices") and MEXT [Innovative Area "Nano Spin Conversion Science" (No. 26103005)]. D. H. was supported by the Yoshida Scholarship Foundation through the Doctor 21 program. M. S. was supported by Grant-in-Aid for Scientific Research on Innovative Area, "Nano Spin Conversion Science" (Grant No. 17H05174) and "Quantum Liquid Crystals" (Grant No. 19H05825) as well as JSPS KAKENHI (Grants No. 17K05513 and No. 15H02117).

*daichihirobe@ims.ac.jp
†masahiro.sato.phys@vc.ibaraki.ac.jp

[1] K. Uchida, H. Adachi, T. Ota, H. Nakayama, S. Maekawa, and E. Saitoh, Observation of longitudinal spin-Seebeck effect in magnetic insulators, Appl. Phys. Lett. **97**, 172505 (2010).

[2] J. Xiao, G. E. W. Bauer, K. Uchida, E. Saitoh, and S. Maekawa, Theory of magnon-driven spin Seebeck effect, Phys. Rev. B **81**, 214418 (2010).

[3] H. Adachi, J. I. Ohe, S. Takahashi, and S. Maekawa, Linear-response theory of spin Seebeck effect in ferromagnetic insulators, Phys. Rev. B **83**, 094410 (2011).

[4] S. S.-L. Zhang and S. Zhang, Spin convertance at magnetic interfaces, Phys. Rev. B **86**, 214424 (2012).

[5] S. Hoffman, K. Sato, and Y. Tserkovnyak, Landau-Lifshitz theory of the longitudinal spin Seebeck effect, Phys. Rev. B **88**, 064408 (2013).

[6] S. M. Rezende, R. L. Rodriguez-Suarez, R. O. Cunha, A. R. Rodrigues, F. L. A. Machado, G. A. Fonseca Guerra, J. C. Lopez Ortiz, and A. Azevedo, Magnon spin-current theory for the longitudinal spin-Seebeck effect, Phys. Rev. B **89**, 014416 (2014).

[7] S. M. Wu, J. E. Pearson, and A. Bhattacharya, Paramagnetic Spin Seebeck Effect, Phys. Rev. Lett. **114**, 186602 (2015).

[8] T. Kikkawa, K. Uchida, S. Daimon, Z. Qiu, Y. Shiomi, and E. Saitoh, Critical suppression of spin Seebeck effect by magnetic fields, Phys. Rev. B **92**, 064413 (2015).

[9] H. Jin, S. R. Boona, Z. Yang, R. C. Myers, and J. P. Heremans, Effect of the magnon dispersion on the longitudinal spin Seebeck effect in yttrium iron garnets, Phys. Rev. B **92**, 054436 (2015).

[10] A. Kehlberger, U. Ritzmann, D. Hinzke, E.-J. Guo, J. Cramer, G. Jakob, M. C. Onbasli, D. H. Kim, C. A. Ross, M. B. Jungfleisch, B. Hillebrands, U. Nowak, and M. Klaui, Length Scale of the Spin Seebeck Effect, Phys. Rev. Lett. **115**, 096602 (2015).

[11] A. Aqeel, N. Vlietstra, J. A. Heuver, G. E. W. Bauer, B. Noheda, B. J. van Wees, and T. T. M. Palstra, Spin-Hall magnetoresistance and spin Seebeck effect in spin-spiral and paramagnetic phases of multiferroic $CoCr_2O_4$ films, Phys. Rev. B **92**, 224410 (2015).

[12] S. Seki, T. Ideue, M Kubota, Y. Kozuka, R. Takagi, M. Nakamura, Y. Kaneko, M. Kawasaki, and Y. Tokura, Thermal Generation of Spin Current in an Antiferromagnet, Phys. Rev. Lett. **115**, 266601 (2015).

[13] S. M. Wu, W. Zhang, A. KC, P. Borisov, J. E. Pearson, J. S. Jiang, D. Lederman, A. Hoffmann, and A. Bhattacharya, Antiferromagnetic Spin Seebeck Effect, Phys. Rev. Lett. **116**, 097204 (2016).

[14] S. Geprags *et al.*, Origin of the spin Seebeck effect in compensated ferrimagnets, Nat. Commun. **7**, 10452 (2016).

[15] J. Li, Y. Xu, M. Aldosary, C. Tang, Z. Lin, S. Zhang, R. Lake, and J. Shi, Observation of magnon-mediated current drag in Pt/yttrium iron garnet/Pt(Ta) trilayers, Nat. Commun. **7**, 10858 (2016).

[16] D. Hirobe, M. Sato, T. Kawamawa, Y. Shiomi, K. Uchida, R. Iguchi, Y. Koike, S. Maekawa, and E. Saitoh, One-dimensional spinon spin currents, Nat. Phys. **13**, 30 (2017).

[17] D. Hirobe, T. Kawamata, K. Oyanagi, Y. Koike, and E. Saitoh, Generation of spin currents from one-dimensional quantum spin liquid, J. Appl. Phys. **123**, 123903 (2018).

[18] C. Liu, S. M. Wu, J. E. Pearson, J. S. Jiang, N. d'Ambrumenil, and A. Bhattacharya, Probing short-range magnetic order in a geometrically frustrated magnet by means of the spin Seebeck effect, Phys. Rev. B **98**, 060415(R) (2018).

[19] Z. Qiu, D. Hou, J. Barker, K. Yamamoto, O. Gomonay, and E. Saitoh, Spin colossal magnetoresistance in an antiferromagnetic insulator, Nat. Mater. **17**, 577 (2018).

[20] A. Azevedo, L. H. Vilela-Leao, R. L. Rodriguez-Suarez, A. B. Oliveira, and S. M. Rezende, DC effect in ferromagnetic resonance: Evidence of the spin-pumping effect, J. Appl. Phys. **97**, 10C715 (2005).

[21] E. Saitoh, M. Ueda, H. Miyajima, and G. Tatara, Conversion of spin current into charge current at room temperature: Inverse spin-Hall effect, Appl. Phys. Lett. **88**, 182509 (2006).

[22] S. O. Valenzuela and M. Tinkham, Direct electronic measurement of the spin Hall effect, Nature (London) **442**, 176 (2006).

[23] J. Sinova, S. O. Valenzuela, J. Wunderlich, C. H. Back, and T. Jungwirth, Spin Hall effects, Rev. Mod. Phys. **87**, 1213 (2015).

[24] X. G. Wen, *Quantum Field Theory of Many-Body Systems* (Oxford University Press, Oxford, 2004).

[25] S. Sachdev, Quantum magnetism and criticality, Nat. Phys. **4**, 173 (2008).

[26] L. Balents, Spin liquids in frustrated magnets, Nature (London) **464**, 199 (2010).

[27] T. Giamarchi, *Quantum Physics in One Dimension* (Oxford University Press, Oxford, 2003).

[28] K. Penc and A. M. Läuchli, *Introduction to Frustrated Magnetism*, edited by C. Lacroix, P. Mendels, and F. Mila (Springer, Berlin, 2011), p. 331.

[29] N. Shannon, T. Momoi, and P. Sindzingre, Nematic Order in Square Lattice Frustrated Ferromagnets, Phys. Rev. Lett. **96**, 027213 (2006).

[30] A. V. Chubukov, Chiral, nematic, and dimer states in quantum spin chains, Phys. Rev. B **44**, 4693(R) (1991).

[31] T. Vekua, A. Honecker, H.-J. Mikeska, and F. Heidrich-Meisner, Correlation functions and excitation spectrum of the frustrated ferromagnetic spin-$\frac{1}{2}$ chain in an external magnetic field, Phys. Rev. B **76**, 174420 (2007).

[32] T. Hikihara, L. Kecke, T. Momoi, and A. Furusaki, Vector chiral and multipolar orders in the spin-$\frac{1}{2}$ frustrated ferromagnetic chain in magnetic field, Phys. Rev. B **78**, 144404 (2008).

[33] J. Sudan, A. Luscher, and A. M. Läuchli, Emergent multipolar spin correlations in a fluctuating spiral: The frustrated ferromagnetic spin-$\frac{1}{2}$ Heisenberg chain in a magnetic field, Phys. Rev. B **80**, 140402(R) (2009).

[34] M. Sato, T. Momoi, and A. Furusaki, NMR relaxation rate and dynamical structure factors in nematic and multipolar liquids of frustrated spin chains under magnetic fields, Phys. Rev. B **79**, 060406(R) (2009).

[35] M. Sato, T. Hikihara, and T. Momoi, Field and temperature dependence of NMR relaxation rate in the magnetic quadrupolar liquid phase of spin-$\frac{1}{2}$ frustrated ferromagnetic chains, Phys. Rev. B **83**, 064405 (2011).

[36] M. Sato, T. Hikihara, and T. Momoi, Spin-Nematic and Spin-Density-Wave Orders in Spatially Anisotropic Frustrated Magnets in a Magnetic Field, Phys. Rev. Lett. **110**, 077206 (2013).

[37] A. A. Nersesyan, A. O. Gogolin, and F. H. L. Eßler, Incommensurate Spin Correlations in Spin-$\frac{1}{2}$ Frustrated Two-Leg Heisenberg Ladders, Phys. Rev. Lett. **81**, 910 (1998).

[38] T. Hikihara, M. Kaburagi, and H. Kawamura, Ground-state phase diagrams of frustrated spin-S XXZ chains: Chiral ordered phases, Phys. Rev. B **63**, 174430 (2001).

[39] S. Furukawa, M. Sato, and S. Onoda, Chiral Order and Electromagnetic Dynamics in One-Dimensional Multiferroic Cuprates, Phys. Rev. Lett. **105**, 257205 (2010).

[40] S. Furukawa, M. Sato, S. Onoda, and A. Furusaki, Ground-state phase diagram of a spin-$\frac{1}{2}$ frustrated ferromagnetic XXZ chain: Haldane dimer phase and gapped/gapless chiral phases, Phys. Rev. B **86**, 094417 (2012).

[41] M. Sato, S. Furukawa, S. Onoda, and A. Furusaki, Competing phases in spin-$\frac{1}{2}$ $J_1 - J_2$ chain with easy-plane anisotropy, Mod. Phys. Lett. B **25**, 901 (2011).

[42] N. Büttgen, P. Kuhns, A. Prokofiev, A. P. Reyes, and L. E. Svistov, High-field NMR of the quasi-one-dimensional antiferromagnet $LiCuVO_4$, Phys. Rev. B **85**, 214421 (2012).

[43] M. Enderle, C. Mukherjee, B. Fåk, R. K. Kremer, J.-M. Broto, H. Rosner, S.-L. Drechsler, J. Richter, J. Malek, A. Prokofiev, W. Assmus, S. Pujol, J.-L. Raggazzoni, H. Rakoto, M. Rheinstädter, and H. M. Rønnow, Quantum helimagnetism of the frustrated spin-$\frac{1}{2}$ chain $LiCuVO_4$, Europhys. Lett. **70**, 237 (2005).

[44] Y. Naito, K. Sato, Y. Yasui, Y. Kobayashi, Y. Kobayashi, and M. Sato, Ferroelectric transition induced by the incommensurate magnetic ordering in $LiCuVO_4$, J. Phys. Soc. Jpn. **76**, 023708 (2007).

[45] L. E. Svistov, T. Fujita, H. Yamaguchi, S. Kimura, K. Omura, A. Prokofiev, A. I. Smirnov, Z. Honda, and M. Hagiwara, New high magnetic field phase of the frustrated $S = \frac{1}{2}$ chain compound $LiCuVO_4$, JETP Lett. **93**, 21 (2011).

[46] M. Hase, H. Kuroe, K. Ozawa, O. Suzuki, H. Kitazawa, G. Kido, and T. Sekine, Magnetic properties of $Rb_2Cu_2Mo_3O_{12}$ including a one-dimensional spin-$\frac{1}{2}$ Heisenberg system with ferromagnetic first-nearest-neighbor and antiferromagnetic second-nearest-neighbor exchange interactions, Phys. Rev. B **70**, 104426 (2004).

[47] K. Matsui, A. Yagi, Y. Hoshino, S. Atarashi, M. Hase, T. Sasaki, and T. Goto, Rb-NMR study of the quasi-one-dimensional competing spin-chain compound $Rb_2Cu_2Mo_3O_{12}$, Phys. Rev. B **96**, 220402(R) (2017).

[48] A. U. B. Wolter, F. Lipps, M. Schäpers, S.-L. Drechsler, S. Nishimoto, R. Vogel, V. Kataev, B. Büchner, H. Rosner, M. Schmitt, M. Uhlarz, Y. Skourski, J. Wosnitza, S. Süllow, and K. C. Rule, Magnetic properties and exchange integrals of the frustrated chain cuprate linarite $PbCuSO_4(OH)_2$, Phys. Rev. B **85**, 014407 (2012).

[49] M. Schäpers *et al.*, Thermodynamic properties of the anisotropic frustrated spin-chain compound linarite $PbCuSO_4(OH)_2$, Phys. Rev. B **88**, 184410 (2013).

[50] K. Nawa, Y. Okamoto, A. Matsuo, K. Kindo, Y. Kitahara, S. Yoshida, S. Ikeda, S. Hara, T. Sakurai, S. Okubo, H. Ohta, and Z. Hiroi, $NaCuMoO_4(OH)$ as a Candidate Frustrated J_1-J_2 Chain Quantum Magnet, J. Phys. Soc. Jpn. **83**, 103702 (2014).

[51] K. Nawa, M. Yoshida, M. Takigawa, Y. Okamoto, and Z. Hiroi, Collinear spin-density-wave order and anisotropic spin fluctuations in the frustrated J_1-J_2 chain magnet $NaCuMoO_4(OH)$, Phys. Rev. B **96**, 174433 (2017).

[52] S. E. Dutton, M. Kumar, M. Mourigal, Z. G. Soos, J.-J. Wen, C. L. Broholm, N. H. Andersen, Q. Huang, M. Zbiri, R. Toft-Petersen, and R. J. Cava, Quantum Spin Liquid in Frustrated One-Dimensional $LiCuSbO_4$, Phys. Rev. Lett. **108**, 187206 (2012).

[53] H.-J. Grafe, S. Nishimoto, M. Iakovleva, E. Vavilova, L. Spillecke, A. Alfonsov, M.-I. Sturza, S. Wurmehl, H. Nojiri, H. Rosner, J. Richter, U. K. Rößler, S.-L. Drechsler, V. Kataev, and B. Büchner, Signatures of a magnetic-field-induced unconventional nematic liquid in the frustrated and anisotropic spin-chain cuprate $LiCuSbO_4$, Sci. Rep. **7**, 6720 (2017).

[54] M. Pregelj, A. Zorko, O. Zaharko, H. Nojiri, H. Berger, L. C. Chapon, and D. Arcón, Spin-stripe phase in a frustrated zigzag spin-$\frac{1}{2}$ chain, Nat. Commun. **6**, 7255 (2015).

[55] M. Enderle, B. Fåk, H.-J. Mikeska, R. K. Kremer, A. Prokofiev, and W. Assmus, Two-Spinon and Four-Spinon

Continuum in a Frustrated Ferromagnetic Spin-$\frac{1}{2}$ Chain, Phys. Rev. Lett. **104**, 237207 (2010).

[56] S.-L. Drechsler, S. Nishimoto, R. O. Kuzian, J. Málek, W. E. A. Lorenz, J. Richter, J. van den Brink, M. Schmitt, and H. Rosner, Comment on "Two-Spinon and Four-Spinon Continuum in a Frustrated Ferromagnetic Spin-$\frac{1}{2}$ Chain", Phys. Rev. Lett. **106**, 219701 (2011).

[57] M. E. Zhitomirsky and H. Tsunetsugu, Magnon pairing in quantum spin nematic, Europhys. Lett. **92**, 37001 (2010).

[58] H. Ueda and K. Totsuka, Magnon Bose-Einstein condensation and various phases of three-dimensional quantum helimagnets under high magnetic field, Phys. Rev. B **80**, 014417 (2009).

[59] A. Orlova, E. L. Green, J. M. Law, D. I. Gorbunov, G. Chanda, S. Krämer, M. Horvatic, R. K. Kremer, J. Wosnitza, and G. L. J. A. Rikken, Nuclear Magnetic Resonance Signature of the Spin-Nematic Phase in $LiCuVO_4$ at High Magnetic Fields, Phys. Rev. Lett. **118**, 247201 (2017).

[60] K. Nawa, M. Takigawa, M. Yoshida, and K. Yoshimura, Anisotropic spin fluctuations in the quasi one-dimensional frustrated magnet $LiCuVO_4$, J. Phys. Soc. Jpn. **82**, 094709 (2013).

[61] N. Büttgen, K. Nawa, T. Fujita, M. Hagiwara, P. Kuhns, A. Prokofiev, A. P. Reyes, L. E. Svistov, K. Yoshimura, and M. Takigawa, Search for a spin-nematic phase in the quasi-one-dimensional frustrated magnet $LiCuVO_4$, Phys. Rev. B **90**, 134401 (2014).

[62] T. Masuda, M. Hagihara, Y. Kondoh, K. Kaneko, and N. Metoki, Spin density wave in insulating ferromagnetic frustrated chain $LiCuVO_4$, J. Phys. Soc. Jpn. **80**, 113705 (2011).

[63] M. Mourigal, M. Enderle, B. Fåk, R. K. Kremer, J. M. Law, A. Schneidewind, A. Hiess, and A. Prokofiev, Evidence of a Bond-Nematic Phase in $LiCuVO_4$, Phys. Rev. Lett. **109**, 027203 (2012).

[64] See Supplemental Material at http://link.aps.org/supplemental/10.1103/PhysRevLett.123.117202 for details on experimental methods, additional data, and theoretical calculations, which includes Refs. [65–77].

[65] S. R. Boona and J. P. Heremans, Magnon thermal mean free path in yttrium iron garnet, Phys. Rev. B **90**, 064421 (2014).

[66] Y. Onose, Y. Shiomi, and Y. Tokura, Lorentz Number Determination of the Dissipationless Nature of the Anomalous Hall Effect in Itinerant Ferromagnets, Phys. Rev. Lett. **100**, 016601 (2008).

[67] Y. Shiomi, Y. Onose, and Y. Tokura, Extrinsic anomalous Hall effect in charge and heat transport in pure iron, $Fe_{0.997}Si_{0.003}$, and $Fe_{0.97}Co_{0.03}$, Phys. Rev. B **79**, 100404(R) (2009).

[68] Y. Shiomi, Y. Onose, and Y. Tokura, Effect of scattering on intrinsic anomalous Hall effect investigated by Lorenz ratio, Phys. Rev. B **81**, 054414 (2010).

[69] Y. Onose, T. Ideue, H. Katsura, Y. Shiomi, N. Nagaosa, and Y. Tokura, Observation of the Magnon Hall Effect, Science **329**, 297 (2010).

[70] D. Hirobe, M. Sato, Y. Shiomi, H. Tanaka, and E. Saitoh, Magnetic thermal conductivity far above the Néel temperature in the Kitaev-magnet candidate α-$RuCl_3$, Phys. Rev. B **95**, 24112(R) (2017).

[71] Y. Shiomi, T. Ohtani, S. Iguchi, T. Sasaki, Z. Qiu, H. Nakayama, K. Uchida, and E. Saitoh, Interface-dependent magnetotransport properties for thin Pt films on ferrimagnetic $Y_3Fe_5O_{12}$, Appl. Phys. Lett. **104**, 242406 (2014).

[72] R. Iguchi, K. Uchida, S. Daimon, and E. Saitoh, Concomitant enhancement of the longitudinal spin Seebeck effect and the thermal conductivity in a Pt/YIG/Pt system at low temperatures, Phys. Rev. B **95**, 174401 (2017).

[73] L. S. Parfen'eva, I. A. Smirnov, H. Misiorek, J. Mucha, A. Jezowski, A. V. Prokof'ev, and W. Assmus, Spinon thermal conductivity of $-(CuO_2)-$ spin chains in $LiCuVO_4$, Phys. Solid State **46**, 357 (2004).

[74] A. M. Zagoskin, *Quantum Theory of Many-Body Systems: Techniques and Applications* 2nd ed.(Springer, New York, 2014).

[75] G. Stefanucci and R. v. Leeuwen, *Nonequilibrium Many-Body Theory of Quantum Systems: A Modern Introduction* (Cambridge University Press, Cambridge, England, 2013).

[76] H. Onishi, Magnetic excitations of spin nematic state in frustrated ferromagnetic chain, J. Phys. Soc. Jpn. **84**, 083702 (2015).

[77] A. A. Abrikosov, L. P. Gorkov, and I. E. Dzyaloshinski, *Methods of Quantum Field Theory in Statistical Physics* (Dover Publications, New York, 1975).

[78] M. Oshikawa, M. Yamanaka, and I. Affleck, Magnetization Plateaus in Spin Chains: "Haldane Gap" for Half-Integer Spins, Phys. Rev. Lett. **78**, 1984 (1997).

[79] M. Oshikawa, Commensurability, Excitation Gap, and Topology in Quantum Many-Particle Systems on a Periodic Lattice, Phys. Rev. Lett. **84**, 1535 (2000).

[80] M. B. Hastings, Lieb-Schultz-Mattis in higher dimensions, Phys. Rev. B **69**, 104431 (2004).

[81] A-P. Jauho, N. S. Wingreen, and Y. Meir, Time-dependent transport in interacting and noninteracting resonant-tunneling systems, Phys. Rev. B **50**, 5528 (1994).

[82] In Eq. (2), the growth of the uniform magnetic moment was represented by the enhancement of the renormalization factor of χ^{-+}_{mag} (see Supplemental Material [64]). In the magnon picture, this enhancement can be regarded as the growth of the angular momentum per single magnon.